Diffusion and Sorption of Benzene Vapor through Polybutadiene-, Polybutadiene/styrene-, and Polybutadiene/acrylonitrile-Based Polyurethanes

Yurun Yang,[1] Yongmin Huang,[2] Yonglin Chen,[1] Dening Wang,[1] Honglai Liu,[2] Chunpu Hu[1]

[1]School of Material Science and Engineering, East China University of Science and Technology, Shanghai, 200237
[2]Department of Chemistry, East China University of Science and Technology, Shanghai, 200237

ABSTRACT: A series of polyurethane (PU) films made from toluene diisocyanate (TDI), 1,4-butanediol (BDO), and hydroxyl-terminated polybutadiene (HTPB), hydroxyl terminated polybutadiene/styrene (HTBS), or hydroxyl terminated polybutadiene/acrylonitrile (HTBN) was synthesized by solution polymerization. The absorption of benzene vapor was found mainly in the soft phase. The equilibrium adsorption (M_∞) was reduced with increasing hard segment content for all the PUs. The values of M_∞ were in the sequence of HTBN-PUs > HTBS-PUs > HTPB-PUs, which could be explained by the different interaction parameters between soft segments and benzene. The HTBN-PU film showed the lowest degree of phase segregation and had more hard segments intermixed in the soft phase, restricting the movement of soft segments, and therefore resulted to non-Fickian behavior, while the HTPB-PU is antithetical. FTIR and atomic force microscopy were utilized to identify the hydrogen bonding behavior and morphology change of the PU films before and after the absorption of benzene vapor. The tensile strength of the HTBN-PUs showed a greater decrease than that of HTBS-PUs and HTPB-PUs after absorbing benzene vapor. © 2004 Wiley Periodicals, Inc. J Appl Polym Sci 91: 2984–2991, 2004

Key words: polyolefin based polyurethane; benzene vapor; diffusion; sorption; morphology

INTRODUCTION

The diffusion and sorption behavior of organic solvent through polyurethane (PU) gained great interest during the past decades[1–9]. This was mainly due to the variety of the morphology of PU and its potential commercial and engineering-oriented applications, including barriers in chemical and food industries and membrane separation. Aminabhavi and Khinnavar[1] studied the diffusion and sorption of C_1-C_5 aliphatic alcohols, halogen-substituted organic penetrants[2], monocyclic aromatics,[3] and some other industrial solvents[4,5] through the PU by immersion/weight gain assay. There were also other reports about sorption of organic liquids in PU by immersion/weight gain assay[6–9]. Investigations on permeation of organic vapor through PU, however, were not reported as much. Most of them dealt with measuring the diffusion of the vapor of water[10], benzene[11,12], dimethy acetamide,[13] etc. These reports paid more attention to sorption behavior, but less to the relationship between the sorption behavior and the structure as well as the morphology of the PU film.

Polyolefin-based PU is a special kind of PU that offers the advantages of low water permeability, good flexibility at low temperature, and biocompatibility. Polybutadiene (HTPB)-based polyurethane is a well-studied type of polyolefin-based PU[14–18] because there is no possibility of hydrogen bonding between its hard and soft segments, which leads to very high degree of phase separation. Fewer studies have been published on the polybutadiene/styrene (HTBS)- and polybutadiene/acrylonitrile (HTBN)-based polyurethanes. These two polyolefin-based polyurethanes offer the advantage of higher mechanical properties. In addition, the influence of the styrene groups and polar acrylonitrile groups in soft segments on the morphology of PU is also attractive. In the present work, the sorption behavior of benzene vapor in a series of polybutadiene/styrene-, polybutadiene/acrylonitrile-, and polybutadiene-based PU films containing different proportions of hard segments are investigated by using a quartz-spring microbalance. Results are then discussed in association with their structure and morphology. The change of morphology and mechanical properties of the polyolefin-based PUs after absorbing benzene vapor are also discussed.

EXPERIMENTAL

Materials

HTBN (M_n = 2400, F_n = 2.0, containing 20.3% of acrylonitrile), HTBS (M_n = 2400, F_n = 2.0, containing
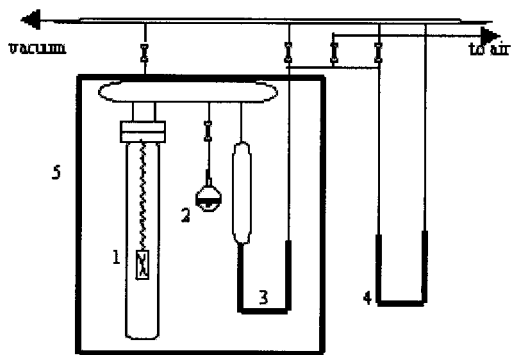
Figure 1 Scheme of the chamber used for absorption study. 1, Quartz spring and PU film; 2, flask for benzene; 3 and 4, U-pressure meter; 5, heater room.

15% of styrene), and HTPB (M_n = 2300, F_n = 2.0), available from Lanzhou Chemical Co., were dewatered under vacuum at 70°C for 8 h before being used. Toluene diisocyanate (TDI, an 80 : 20 mixture of 2,4 and 2,6 isomers) and dibutyltin dilaurate (DBTDL) were used as received. 1,4-Butadiol (1,4-BDO), tetrahydrofuran (THF), ethyl acetate, and benzene were purified by distillation.

Preparation of PU films

The NCO-terminated PU prepolymers were prepared by reacting each of the above polyolefin-based polyols with TDI (1 : 2 by mol) in the presence of ethyl acetate as solvent at 70°C. The reaction proceeded until the theoretical content of –NCO groups was reached. The prepolymer was then chain extended with 1,4-BDO by using DBTDL (0.02 wt % of polyol) as catalyst. The resultant was diluted with THF to 30% of solid content. Each PU solution was poured onto a glass plate to form a film with a thickness of about 100 μm. The solvent in the film was removed by evaporation at 70°C for 12 h at first, and then under vacuum at the same temperature for 1 week more. The PU films were peeled from the glass plates after they had been immersed in deionized water for several hours and were dried thereafter and then stored for 1 month.

Sorption experiment

The equipment used for studying the sorption of benzene vapor in PU films was based on the gravimetric measurement technique. The scheme of the sorption chamber with its accessories is shown in Figure 1[19]. The temperature of the whole chamber was controlled to be 35 ± 0.5°C during sorption experiments. PU film was hung from the spring in the sorption chamber. The chamber was evacuated and then filled with the saturated vapor of benzene. The sensitive quartz spring was used to follow the variation of the weight of the film with time during the sorption. The time–weight data were used to calculate the diffusion coefficient (D).

The diffusion coefficient (D) was calculated in accordance with the Fickian equation[5]. If the diffusion follows the Fickian mechanism, the integrated Fickian equation yields as follows:

$$\frac{M_t}{M_\infty} = \frac{4}{\pi^{1/2} l} (Dt)^{1/2} \tag{1}$$

where M_t and M_∞ represent the amount of absorbed benzene vapor (in g) by 1 g of PU film (percentage mass uptake) at time t and at the time when the absorption reaches the equilibrium, i.e., the maximum absorption, respectively; and l is the thickness of the film. The value of D can be determined by l and the slope R of the initial linear portion of sorption curve M_t/M_∞ versus $t^{1/2}$ by using eq. (2) derived from the eq. (1).

TABLE I
DSC Results and Sorption Data of PU Films

Sample	Type of soft segment	Hard segment content (wt %)	$T_g s_0$ (°C)	$T_g s$ (°C)	$T_g s - T_g s_0$ (°C)	W_{ss} (%)	$D \times 10^{12}$ (m^2/s)	M_∞ (g, benzene/g, polymer)
BN1	HTBN	24.9	−44.4	−29.5	14.9	81.9	*	0.50
BN2	HTBN	36.7	−44.4	−32.7	11.7	85.6	*	0.43
BN3	HTBN	51.9	−44.4	−33.4	11.0	86.4	*	0.30
BN4	HTBN	62.9	−44.4	−31.5	12.9	84.2	*	0.23
BS1	HTBS	24.8	−68.3	−62.4	5.9	93.1	*	0.44
BS2	HTBS	36.9	−68.3	−62.7	5.6	93.5	*	0.43
BS3	HTBS	51.1	−68.3	−63.2	5.1	94.0	*	0.28
BS4	HTBS	62.0	−68.3	−63.3	5.0	94.1	*	0.20
B1	HTPB	24.8	−77.9	−74.3	3.6	95.8	7.6	0.40
B2	HTPB	37.2	−77.9	−72.8	5.1	94.1	4.9	0.39
B3	HTPB	51.1	−77.9	−74.9	3.0	96.5	3.4	0.25
B4	HTPB	62.1	−77.9	−74.4	3.5	95.6	3.4	0.19

* Non-Fickian behavior.

TABLE II
Solubility Parameters and Polymer–Benzene Interaction
Parameters for Polyolefine-Based PUs

Material	δ ($J^{1/2}/cm^{3/2}$)	x (with benzene)
HTBN	19.3	0.36
HTBS	17.4	0.39
HTPB	17.0	0.43
TDI-BDO	25.3	2.11
Benzene	18.6	—

$$D = \left(\frac{\pi}{16}\right)(Rl)^2 \qquad (2)$$

If the diffusion does not follow the Fickian mechanism, then the degree of deviation from the Fickian behavior could be calculated in accordance with the empirical expression[20].

$$\frac{M_t}{M_\infty} = kt^n \qquad (3)$$

where n and k are related to the diffusion behavior and the degree of polymer–benzene interaction, respectively. The parameters n and k could be determined by least square fit of $\log(M_t/M_\infty)$ versus $\log t$.

Instrument measurement

Differential scanning calorimetry (DSC; NETZSCH-Geratebau GmbH Thermal Analysis) was used to measure the glass transition temperatures, and the temperature of the sample cell was controlled within a range between -150 and $200°C$; the heating rate was $20°C/min$. ATR-FTIR spectra were obtained from the NICOLET 5DX equipment. Atomic force microscopy (AFM; Digital III of Digital Instruments Co.) was used to observe the morphology of the PU films by tapping mode. The mechanical properties were measured by the Instron 4465 instrument at the stretch rate of 100

TABLE III
Values of n and k for Diffusion Behavior of PUs

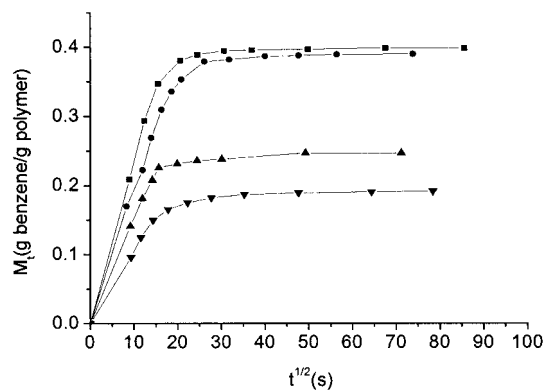| Sample	n	$k \times 10^2$
BN1	0.95	0.41
BN2	0.98	0.36
BN3	1.00	0.03
BN4	1.24	0.04
BS1	0.56	4.0
BS2	0.57	3.2
BS3	0.56	3.4
BS4	0.66	2.4
B1	0.47	7.0
B2	0.48	6.7
B3	0.48	6.6
B4	0.52	5.1

Figure 2 Benzene vapor absorption M_t versus square root of time for HTPB-based PU films (■) B1; (●) B2; (▲) B3; (▼) B4.

mm/min. The dimension of every PU film was about $120 \times 10 \times 0.1$ mm.

RESULTS AND DISCUSSION

Relationship between the structure, morphology, and equilibrium absorption as well as diffusion coefficient

The DSC results and sorption data of a series of HTBN-, HTBS-, and HTPB-based PUs with different hard segment contents are listed in Table I. From Table I, it can be seen that the values of M_∞ reduce with the increase of hard segment content for all the PU films. This could suggest that the absorption of nonpolar benzene vapor was mainly in the soft phase.

The approximate values of solubility parameters(δ) and polymer–benzene interaction parameters (x) in Table II, calculated by the method of group contribu-
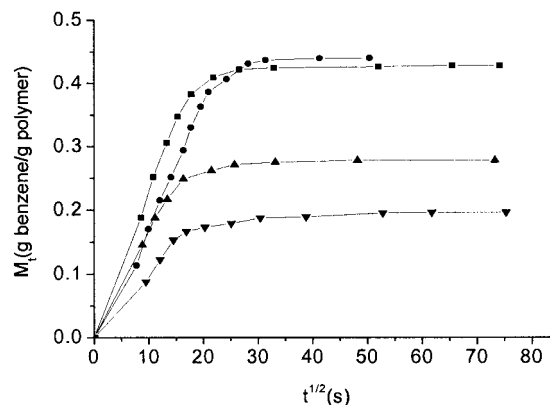
(■) B1; (●) B2; (▲) B3; (▼) B4.

Figure 3 Benzene vapor absorption M_t versus square root of time for HTBS-based PU films (■) BS1; (●) BS2; (▲) BS3; (▼) BS4.
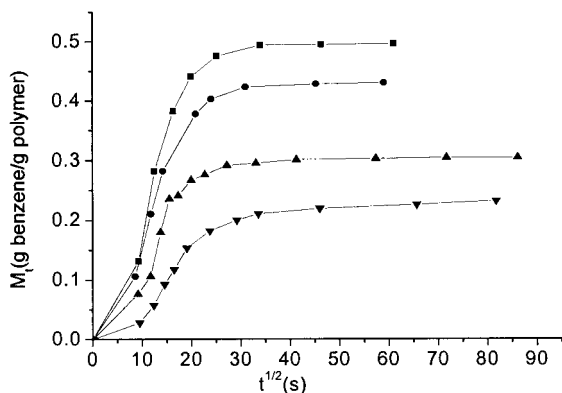
Figure 4 Benzene vapor absorption M_t versus square root of time for HTBN-based PU films (■) BN1; (●) BN2; (▲) BN3; (▼) BN4.

tion[21] and according to the theory of solubility parameter[22], could support the above deduction. The solubility parameter of the benzene vapor is very close to those of the three types of the soft segments but differs greatly from that of the hard segment. The values of x between the hard segment (TDI-BDO) and benzene are far greater than 0.5, indicating the good resistance of the hard segments against benzene and the weak interaction between them. The values of x between the soft segments and benzene are below the critical value of 0.5, which means that the soft segments were miscible with benzene.

Comparing the values of M_∞ of HTBN-, HTBS-, and HTPB-based PU films containing the same amount of hard segments in Table I, it is clear that the HTBN-based PU exhibits the largest value, while the HTPB-based PU exhibits the smallest. These results could be well explained by their polymer–benzene interaction parameters (x) in Table II. The value of x between HTBN soft segments and benzene is smallest (0.36), while the value of x between HTPB soft segments and

benzene is greatest (0.43). This suggests that the HTBN soft segment has the greatest interaction with benzene and therefore results in the highest equilibrium adsorption of benzene, while the HTPB is antithetical.

It is well known that the diffusion behavior should be related to the motion ability of macromolecular chains. The extent of hard segments mixed in soft phase, i.e., the degree of phase segregation in PU could greatly influence the motion ability of soft segments and therefore affect the diffusion behavior. The degree of microphase separation of polyolefin-based PU could be judged by the content of pure soft segments in the soft phase (W_{ss}) in Table I calculated by the Fox equation[23]:

$$\frac{1}{T_g s} = \frac{W_{ss}}{T_g s_0} + \frac{(1 - W_{ss})}{T_g h_0} \qquad (4)$$

where $T_g s$, $T_g s_0$, and $T_g h_0$ represent the glass transition temperature of the soft phase in PU, the pure soft segment, and the pure hard segment, respectively. The value of $T_g h_0$ of the pure hard segment consisting of 1,4-BDO and TDI is 72°C[18]. In the present work, the values of W_{ss} for the films of HTBS- and HTPB-based PUs were 0.93–0.94 and 0.94–0.97, indicating that their soft phase contained a small amount of hard segments, but the W_{ss} values of HTBS-based PUs were slightly smaller than those of HTPB-based PUs. The values of W_{ss} of HTBN-based PUs in the present work were 0.81–0.86. These data indicate the difference between the degree of microphase separation in HTPB-, HTBS-, and HTBN-based PUs. The obviously lower degree of microphase separation in HTBN-based PUs might be attributed to the –CN groups in the soft segments, which could form hydrogen bonds with the –NH groups in hard segments, leading to easier mixing of soft and hard segments. The styrene structure in the HTBS could slightly restrain the movement ability of the soft segments and their separation from the hard segments, resulting in a slightly lower degree of microphase separation than that of HTPB-based PU.

To investigate the diffusion mechanism further, the data of dynamic sorption of benzene in polyolefin-based PUs for a short time ($M_t/M_\infty < 0.6$) were substituted into eq. (3), and the results are listed in Table III. If $n = 0.5$, the diffusion follows the Fickian law[24]. It would be not in agreement with Fickian behavior when n is greater than 0.5. The greater the value of n, the larger the degree of deviation from Fickian behav-

TABLE IV
FTIR Results of the Bonded Carbonyl Groups for HTBN-, HTBS-, and HTPB-Based PUs

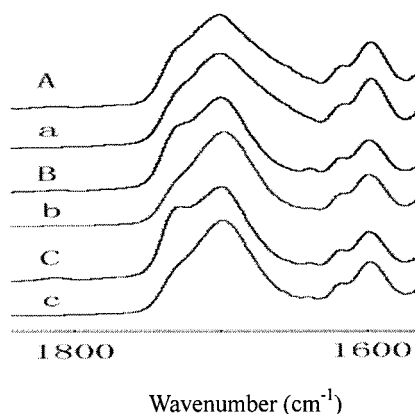| Sample	BN4	BBN4	BS4	BBS4	B4	BB4
X_b	0.84	0.84	0.90	0.81	0.91	0.83

Figure 5 FTIR spectra between the range of 1,600 to 1,800 cm⁻¹ for different PU films before and after benzene absorption: A, BBN4; a, BN4; B, BB4; b, B4; C, BBS4; c, BS4.
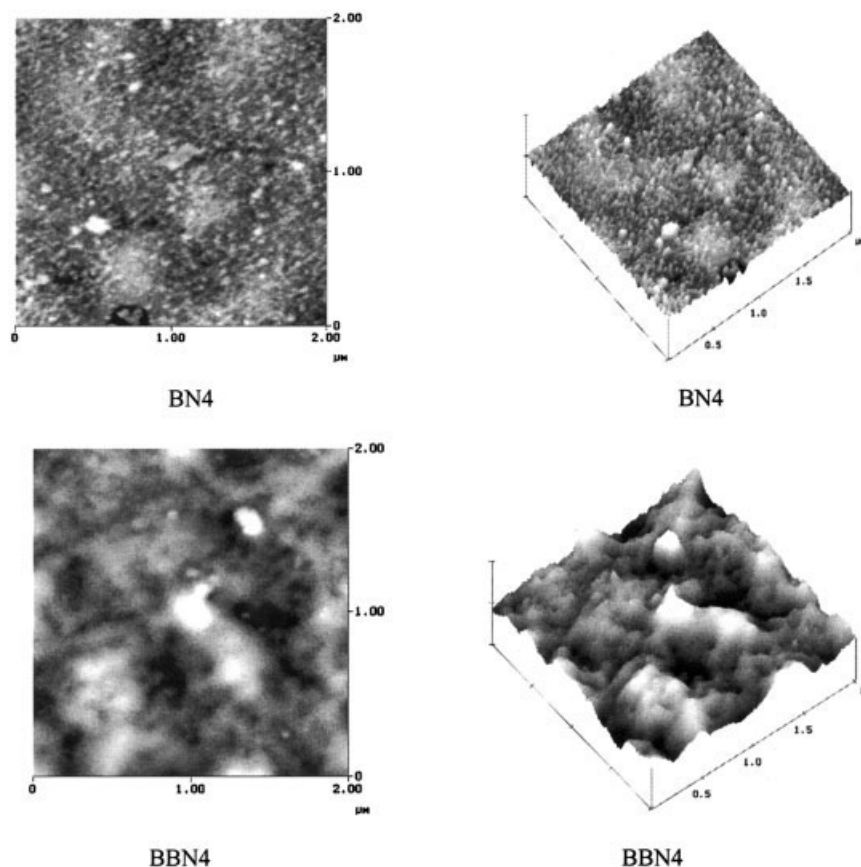
Figure 6 AFM images of HTBN-based PU film before and after benzene absorption.

ior should be. In addition, a larger value of *n* means lower motion ability of the macromolecular chains[24]. The values of *n* for HTBN-based PUs varied from 0.95 to 1.24, indicating their low ability of chain motion. The values of *n* for HTBS-based PUs varied from 0.56 to 0.66, slightly deviated from Fickian behavior. The values of *n* for HTPB-based PUs (0.48 to 0.52) were very close to 0.5, indicating nearly normal Fickian behavior and the highest ability of chain motion among the three types of polyolefin-based PUs. For the majority of the samples, increase of the content of hard segments led to an increase in the value of *n*, namely greater deviation from the Fickian diffusion.

The values of *k* indicate the degree of polymer–benzene interaction. There was a regular trend of the values *k*, i.e., with the increase of the content of hard segments, the value *k* decreased. This suggested that increasing the content of hard segments improved the resistant ability of polyolefin-based PUs against benzene. The order of *k* values for the three types of polyolefin-based PUs was HTBN-PU < HTBS-PU < HTPB-PU, which is in accordance to the result of polymer–benzene interaction parameters (*x*).

According to the above discussion, it can be seen that all of the HTBN- and HTBS-based PUs exhibit non-Fickian behavior, while the HTPB-based PUs show Fickian behavior. The order of *n* values is HTBN- > HTBS- > HTPB-based PUs, when they contain the same amount of hard segments. The reason was that the lower degree of phase separation resulted in a larger amount of hard segments mixed in soft phase, which restricted the movement of soft segments and led to greater deviation from Fickian behavior. In addition, it is clear that increasing the content of hard segments could also restrict the motion of the macromolecular chains, leading to larger value of *n*.

The sorption plots (i.e., M_t versus square root of time, $t^{1/2}$) at 35°C for the HTPB-, HTBS-, and HTBN-based PU films are given in Figures 2–4. For Fickian diffusion, the curve should be linear during the early stage of sorption and then reach a plateau. From Figure 2, it can be seen that the HTPB-based PUs exhibit approximate Fickian diffusion. The sorption plots of HTBS- and HTBN-based PUs in Figures 3 and 4, however, are sigmoid, implying a non-Fickian mechanism.

FTIR study

FTIR was utilized in this paper to discuss the change of morphology of the polyolefin-based PU films before and after absorption of benzene vapor. Here, the films
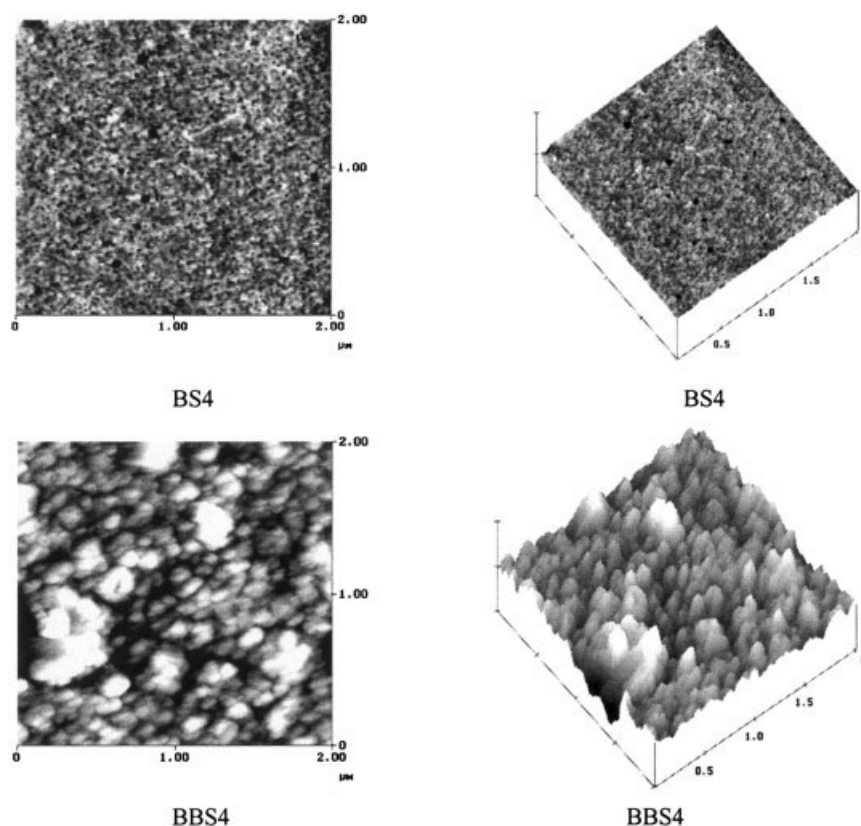
Figure 7 AFM images of HTBS-based PU film before and after benzene absorption.

that reached the equilibrium adsorption are marketed by adding a "B" before the sample code. For example, BBN4 refers to the equilibrium-absorbed film of the sample BN4. The characteristic absorption peaks of carbonyl group in the hard segments between 1,800 and 1,600 cm^{-1} are shown in Figure 5. Multiple absorption peaks can be observed. The peak due to hydrogen-bonded C=O stretching vibration is centered at about 1,700 cm^{-1} and that due to free C=O stretching vibration is centered at about 1,733 cm^{-1}[15]. By separating these two peaks[25], the degree of hydrogen bonding of carbonyl group (X_b) could be calculated:

$$X_b = \frac{\text{Area(bonded)}}{\text{Area(bonded)} + \text{Area(free)}} \quad (5)$$

The values of X_b calculated for the samples BN4, BS4, and B4 before and after benzene vapor absorption are listed in Table IV. From Figure 5 and Table IV, it can be seen that the sample BN4 shows the lowest X_b compared with those of the samples BS4 and B4. The lowest degree of hydrogen bonding of C=O in the hard segments of the HTBN-based PUs implies also the lowest degree of microphase separation, which is well in accordance with the above results of DSC.

Figure 5 and Table IV show that the area of the free C=O absorption bands increases and X_b decreases after absorbing the benzene vapor for HTBS- and HTPB-based PUs, meaning that part of the hydrogen bonds of C=O groups were broken up. It was proven above that the sorption was confined mainly to the soft phase and not obviously affected the glassy hard segment phase, therefore, it could be hypothesized that the destroyed hydrogen bonds of carbonyl groups mainly existed at the interface between hard and soft phase. The value X_b of HTBN-based PUs in Table IV does not change after benzene absorption, which could be related to the lowest value of x for the HTBN–benzene interaction parameter in Table II. Furthermore, the HTBN-based PU not only had the hydrogen bonding between the C=O and the NH groups, but also between the CN and the NH groups. When the soft phase of the HTBN-based PU was swelled by the benzene vapor, the hydrogen bonds between the CN and the NH groups were more easily broken up, which enabled part of the hydrogen bonds to form between the C=O and the NH groups. Similar phenomenon was also proved by other reports[26,27] in which it was discovered and discussed that stronger hydrogen bonds were formed during the breaking of weaker hydrogen bonds.
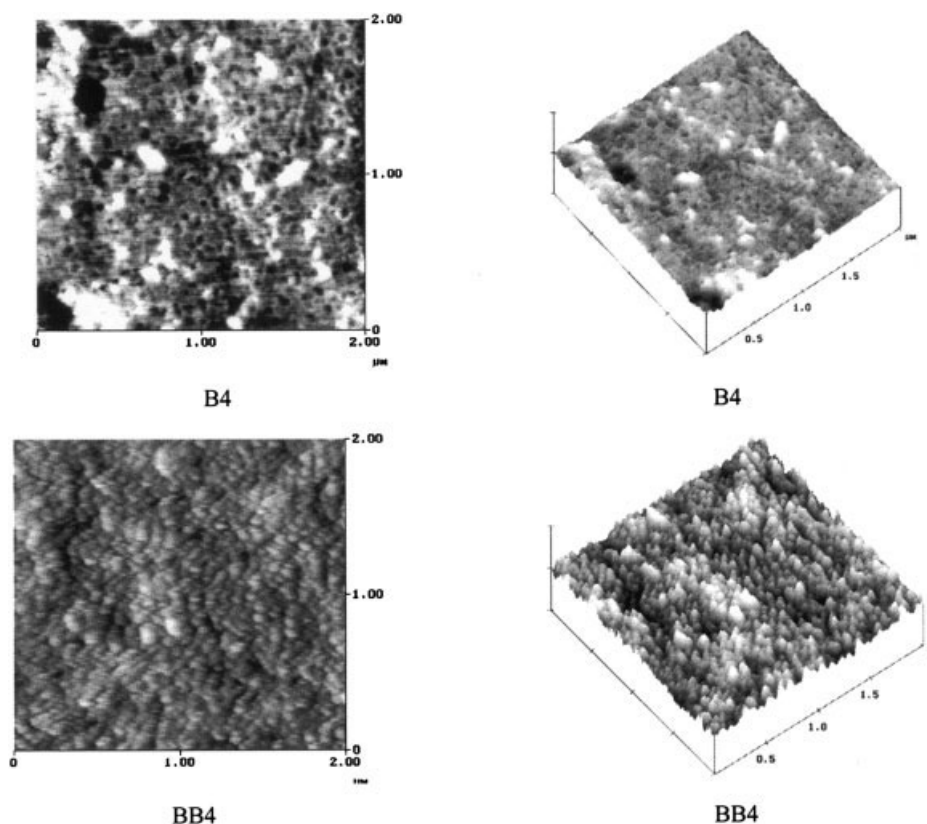
Figure 8 AFM images of HTPB-based PU film before and after benzene absorption.

AFM study

AFM has been proven to be a suitable tool for investigation of the surface morphology of polymers[28]. The images by tapping mode for samples BN4, BS4, and B4 before and after benzene absorption are shown in Figures 6-8. The bright areas correspond to the hard phase, while the dark areas correspond to the soft phase.

For all three types of PUs, large increments in phase dimensions can be seen in Figures 6–8 after the films absorb the benzene vapor, proving that the swelling of the soft phase greatly increased the motion ability of the molecular chains and led to phase recongregation. The degree of the increase of phase dimension shown in Figures 6–8 is in the sequence HTBN > HTBS > HTPB, which is in accordance with the sequence of the values of equilibrium absorption (M_∞). This should imply that higher equilibrium adsorption led to higher chain motion capability and therefore a higher degree of phase recongregation.

Mechanical properties

The mechanical properties of some HTBN-, HTBS-, and HTPB-based PU films before and after benzene absorption are listed in Table V. The tensile strengths of HTBN- and HTBS-based PUs are about 2.2–2.7 and 1.3–1.6 times higher than those of corresponding HTPB-based PUs, respectively. The elongation of the two former types of PUs is also higher than that of HTPB-based PUs. This could be attributed to the reinforcement of the CN polar groups and rigid styrene groups in the soft segments. What is more, the introduction of the CN polar groups cannot only increase the cohesive energy density of soft segments but also form hydrogen bonds with hard segments and there-

TABLE V
Mechanical Properties of Polyolefin-Based PU Films

Sample	BN1	BBN1	BS1	BBS1	B1	BB1	BN4	BBN4	BS4	BBS4	B4	BB4
Tensile strength (Mpa)	15.6	9.6	7.8	6.0	5.8	4.6	41.0	28.8	29.4	23.7	19.2	15.5
Retention of tensile strength (%)		61.5		76.9		79.3		70.2		80.8		80.9
Elongation(%)	300	340	270	280	200	230	100	140	100	120	70	80

fore leads to a remarkable improvement of the mechanical properties. For all three types of PUs, the tensile strengths increase and elongations decrease with increasing content of hard segments.

From Table V, it can be seen that the HTBN-based PUs show the greatest decrease of tensile strength, while the HTPB-based PUs show the least after benzene absorption. This tendency is more obvious when the samples have lower content of hard segments, indicating that soft segments mainly determine the effect of benzene vapor absorption on the mechanical properties of PUs. The greatest loss of tensile strength of the HTBN-based PUs after benzene uptake might mainly result from the breakage of hydrogen bonds between the CN groups and the NH groups as well as the reduction of the cohesive energy density caused by the barrier of nonpolar benzene vapor. The loss of tensile strength of the HTBS- and HTPB-based PUs are lower than those of HTBN-based PUs, implying that the smaller values of M_∞ do not so obviously destroy their framework.

References

1. Aminabhavi, T. M.; Khinnavar, R. S. Polymer 1993, 34, 1006.
2. Aithal, U. S.; Aminabhavi, T. M. J Membr Sci 1990, 50, 225.
3. Aithal, U. S.; Aminabhavi, T. M. Polym Preprints 1989, 30, 17.
4. Aithal, U. S.; Aminabhavi, T. M. J Appl Polym Sci 1991, 42, 2837.
5. Aithal, U. S.; Aminabhavi, T. M.; Balundgi, R. H.; Shukla, S. S. J Macromol Sci Rev Macromol Chem Phys 1990, C30, 43.
6. Liao, D. C.; Chern, Y. C.; Han, J. L.; Hsiesh, K. H. J Polym Sci B Polym Phys 1997, 35, 1747.
7. Enneking, L.; Heintz, A.; Lichtenthaler, R. N. J Membr Sci 1996, 115, 161–170.
8. Schneider, N. S.; Illinger, J. L.; Cleaves, M. A. Polym Mater Sci Eng 1983, 49, 244.
9. Desai, S.; Thakore, M.; Devi, S. Polym Int 1998, 47, 172.
10. Landro, L. D.; Pegoraro, M; Bordogna, L. J Membr Sci 1991, 64, 229.
11. Grabczyk, A. W.; Smigasiewicz, S.; Muszynski, J. Polym Bull 1998, 40, 591.
12. Ponangi, R.; Pintauro, P. N. J Membr Sci 1998, 144, 25.
13. Gou, M. M.; Koros, W. J.; Goldman, G. W. J Appl Polym Sci 1991, 43, 1991.
14. Schneider, N. S.; Brunette, C. M.; Hsu, S. L.; Macknight, W. J. Adv Urethane Sci Technol 1981, 8, 49.
15. Brunette, C. M.; Hsu, S. L.; Macknight, W. J.; Schneider, N. S. Polym Eng Sci 1981, 21, 163.
16. Brunette, C. M.; Hsu, S. L.; Rossman, M.; Macknight, W. J.; Schneider, N. S. Polym Eng Sci 1981, 21, 668.
17. Xu, M.; Macknight, W. J.; Chen, C. H. Y.; Thomas, E. L. Polymer 1983, 24, 1327.
18. Cuve, L.; Pascault, J. P.; Boiteux, G.; Seytre, G. Polymer 1991, 32, 343.
19. Li, J.; Xu, Z. L.; Liu, H. L. J Chem Ind Eng 1997, 48, 517.
20. Brandrup, J.; Immrgut, E. H.; Grulke, E. A., Eds. Polymer Handbook, 4th ed. Wiley: New York, 1999.
21. Bristow, G. M.; Watson, W. F. Trans Faraday Soc 1958, 54, 1731.
22. Fox, T. G. Bull Am Phys Soc 1956, 1, 123.
23. Chiou, J. S.; Paul, D. R. Polym Eng Sci 1968, 26, 1218.
24. Frisch, H. L. Polym Eng Sci 1980, 20, 2.
25. Ning, L.; Wang, D. N.; Ying, S. K. Polymer 1996, 37, 3577.
26. Ning, L.; Wang, D. N.; Ying, S. K. Macromolecules 1997, 30, 4405.
27. Ning, L.; Wang, D. N.; Ying, S. K. Acta Polymerica Sinica 1996, 4, 423.
28. Reifer, D.; Windeit, R.; Kumpf, R. J.; Karbach, A.; Fuchs, H. Thin Solid Films 1995, 264, 148.